Carbon Nanotubes on Polymeric Microcapsules: Free-Standing Structures and Point-Wise Laser Openings

By *Alexey M. Yashchenok, Daniil N. Bratashov, Dmitry A. Gorin,* Maria V. Lomova, Anton M. Pavlov, Andrei V. Sapelkin, Bong Sup Shim, Gennady B. Khomutov, Nicholas A. Kotov, Gleb B. Sukhorukov, Helmuth Möhwald,* and *Andre G. Skirtach*

Single-wall carbon nanotubes modified by anionic polyelectrolyte molecules are embedded into the shells of microcapsules. Carbon nanotubes serve as rigid rods in a softer polymeric capsule, which forms a free-standing shell upon treatment with glutaraldehyde and subsequent drying. The embedded carbon nanotubes exhibit a broad absorption in the UV–near-infrared part of the spectrum, and that allows point-wise activation and opening of the microcapsules by laser. Raman signal analysis shows changes of carbon-nanotube-specific lines after high-power laser irradiation, which is characteristic of the formation of disordered carbonlike structures. These polyelectrolyte/carbon nanotube composite capsules represent a novel light-addressable type of microcontainers.

1. Introduction

Since their discovery by Iijima in 1991 carbon nanotubes are becoming one of the most promising types of materials for nanotechnology.[1,2] They show great promise as materials of choice for surface functionalization enhancing mechanical properties of materials,[3–10] nanoelectronics,[11,12] catalysis,[13–15] diagnostics[16,17] and drug delivery.[18–19] Exceptional mechanical and optical properties of carbon nanotubes make them attractive candidates as functional blocks in molecular assemblies. Incorporation of carbon nanotubes into supramolecular structures is also of great interest to a broad field of nanostructured materials.[20] Recently nano-engineered multilayer structures incorporating carbon nanotubes have been also fabricated by the layer-by-layer self-assembly (LbL).[8–10] This led to fabrication of multifunctional nano-structured polymeric materials with tunable properties.[21,22]

The LbL assembly is based on the sequential adsorption of charged species onto oppositely charged surfaces. By consecutive adsorption steps one is able to build multilayers based on electrostatic interactions. LbL coating of a sacrificial colloidal template can be followed by the dissolution of the template thus producing hollow polyelectrolyte capsules.[23,24] Due to the modularity of the LbL technique it is possible to fabricate tailor-made capsules with multifunctional[25] or stimuli responsive[26,27] walls which can be used in drug-delivery applications.[28,29] Recently the remote activation of microcapsules containing noble metal nanoparticles has been demonstrated.[25–31] To-date, numerous studies focused on microcapsules containing gold nanoparticles.[27–29] Remote release and polyelectrolyte multilayer capsule permeability control due to laser-nanoparticle interaction leads to release of encapsulated materials, and this can be performed inside living cells. This method has already been demonstrated as an important tool in molecular biology.[28–30] For example, we have shown[30] that signal peptides intracellularly released by near-IR irradiation,[31] are bound to the major histocompatibility complex (MHC) Class I molecules and transported to the surface of cells. The complex presentation on the cell surface

---

[*] Dr. A. M. Yashchenok, D. N. Bratashov, Dr. D. A. Gorin, M. V. Lomova, A. M. Pavlov
Faculty of Nano- and Biomedical Technologies
Saratov State University
Saratov, 410012 (Russia)
E-mail: gorin@mpikg.mpg.de

Dr. D. A. Gorin
Department of Interfaces
Max-Planck Institute of Colloids and Interfaces
Golm/Potsdam, D14476 (Germany)

A. M. Pavlov, Prof. G. B. Sukhorukov
School of Engineering & Materials Science
Queen Mary University of London
Mile End Road, London, E1 4NS (UK)

Dr. A. V. Sapelkin
Department of Physics, Queen Mary University of London
Mile End Road, London, E1 4NS (UK)

B.S. Shim, Prof. N. A. Kotov
Department of Chemistry, University of Michigan
Ann Arbor, MI 48109 (USA)

Prof. G. B. Khomutov
Faculty of Physics, Moscow State University
Moscow, 119899 (Russia)

Prof. G. B. Khomutov
Institute of Nanotechnologies for Microelectronics
Leninsky Pr. 32a, Moscow 119991 (Russia)

Prof. H. Möhwald, Dr. A. G. Skirtach
Department of Interfaces
Max-Planck Institute of Colloids and Interfaces
Golm/Potsdam, D14476 (Germany)

DOI: 10.1002/adfm.201000846

is a necessary condition for T-cell recognition and response. Remote release by a biologically friendly near-IR laser is the key component enabling this application.[31]

It was shown in Ref.[39,40] that uptake of microcapsules by living cells is accompanied by a strong pressure exerted on their shells and external pressure can release the content of the microcapsules.[34] This necessitates development of microcapsules with a high mechanical stability. Embedding gold nanoparticles in the microcapsule shell resulted in improved mechanical properties,[32] while enhancement of the stiffness and tensile strength of LbL films containing carbon nanotubes has been demonstrated for planar films.[8–10] This makes carbon nanotubes attractive candidates as constituent component of microcapsule shells. Several studies have reported fabrication of LbL coated spherical colloids with carbon nanotubes.[35–38] Other types of capsules have been also functionalized with carbon nanotubes;[39,40] including remote activation by laser light of capsules with encapsulated nanotubes.[40] In Ref.[40] full destruction of microcapsules loaded by carbon nanotubes after laser irradiation was shown. To the best of our knowledge, no free-standing structure formation and no point-wise remote activation, no Raman analysis and no AFM study of LbL microcapsules with carbon nanotubes in the shell before and after laser irradiation have been reported. However, there is a great need for microscopic understanding of precision addressing in the design of new polymeric capsules with remote release capabilities and enhanced mechanical stability.

Here we report on incorporation of carbon nanotubes into the shells of polyelectrolyte microcapsules. CNTs are rigid rods in the microcapsule shell; we used glutaraldehyde as an additional curing agent to design free-standing microcapsules, i.e. those which do not collapse into flat “pancake”-like structures upon drying. That property is used for enhancement of strength and handling of microcapsules. Broad absorption of CNT in visible – near-IR part of spectrum induces responsiveness to lasers operating in this broad wavelength range. We further used Raman spectroscopy to investigate the influence of laser irradiation on the nanocomposite microcapsule shell.

2. Results and Discussion

Preparation of capsules followed the established process of LbL deposition onto microparticles (**Figure 1**). In the first step, carbon nanotubes are suspended in water and adsorbed onto polyelectrolyte multilayer (PEM) capsules. Atomic force microscopy (AFM) images of carbon nanotubes before adsorption on colloidal templates (Figure 1b) show typical nanotube network morphology with wire-like structures. The aspect ratio is very large (the lengths of carbon nanobutes typically span the millimeter scale, while their diameter of only a few nanometers). In our case, they were functionalized and stabilized with poly(sodium 4-styrenesulfonate) (PSS). Therefore, adsorption of carbon nanotubes was performed onto the poly(allylamine hydrochloride) (PAH) terminated surface (Figure 1c). SEM images of a microparticle template with polyelectrolyte multilayers with and without CNTs reveal important differences in surface topology (**Figure 2**). In

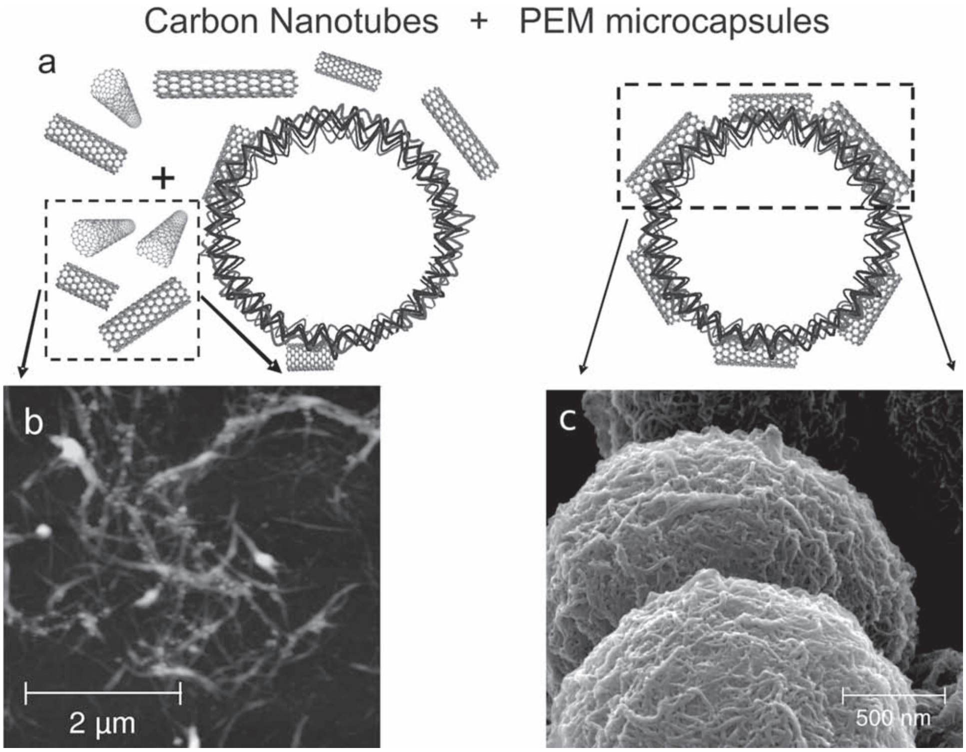

Figure 1. Schematic representation of the carbon nanotube/polyelectrolyte microcapsule assembly (a). AFM images of carbon nanotubes (b) and SEM image of microcapsules with carbon nanotubes in the shell and after glutaraldehyde treatment (c) are shown in the bottom row.

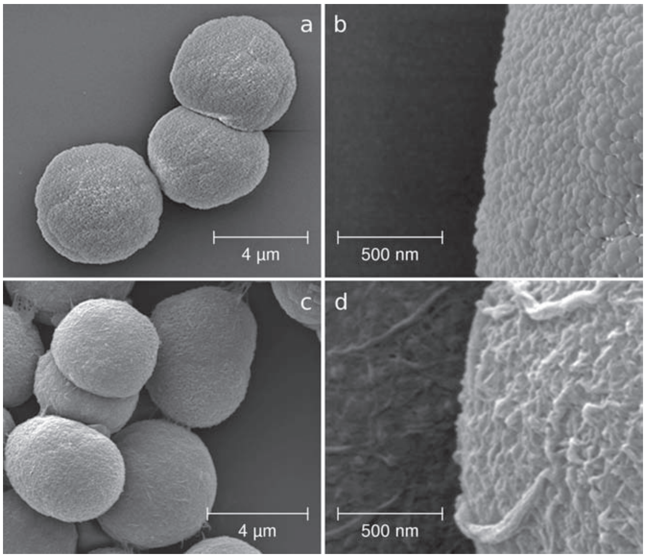

Figure 2. SEM images of microparticle cores with different coating: a,b) polyelectrolyte layer images with different magnification; c,d) carbon nanotube/polyelectrolyte layer images.

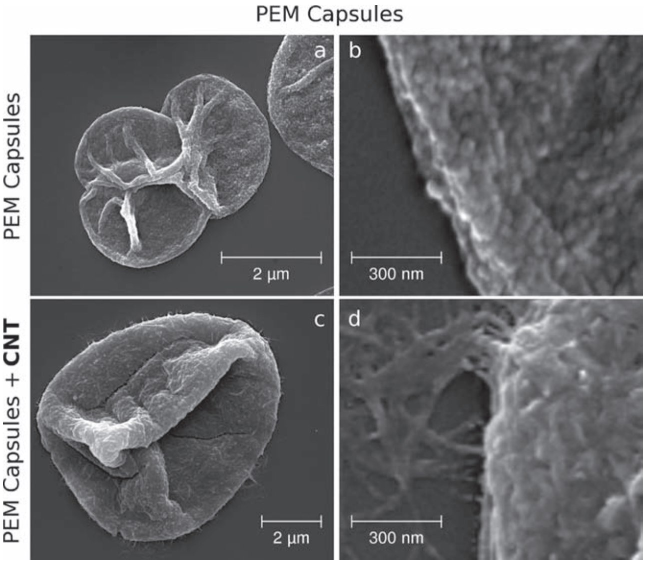

Figure 4. SEM images of polyelectrolyte microcapsules without (a,b) and with carbon nanotubes (c,d).

contrast to the rather smooth surface in absence of CNT (Figure 2a,b) the incorporation of CNT yields a rougher and a network-like structure (Figure 2c,d). The network can be seen in TEM images of the microcapsules (**Figure 3**) produced after the core dissolution.

Figure 4 a,b shows completely collapsed (flat pancake-like) structures of as-prepared microcapsules without carbon nanotubes. This is consistent with earlier observations.[28] Figure 4c,d demonstrates thicker folds and some carbon nanotube aggregates on the surface of microcapsules. Further the influence of glutaraldehyde treatment on the PEM capsules with and without carbon nanotubes was studied by SEM (**Figure 5a–d**). Glutaraldehyde treatment is typically used in biology for fixing cells in order to preserve their morphology on drying and in our case leads to cross-linking of amino groups of cationic polyelectrolytes.[41] A striking difference between untreated and treated with glutaraldehyde capsules was observed. For example, Figure 5a,b shows that PEM microcapsules never collapse into flat "pancake"-like structures, but form some dimples in the middle. Importantly, 70% of polyelectrolyte multilayer capsules with single wall carbon nanotubes maintain their spherical shape and do not collapse after drying in air, Figure 5c,d (Supporting Information). This makes examination of the capsules using SEM much more informative as far as the details of the nanotube inclusion into the capsules are concerned.

The UV – near-IR spectrum of carbon nanotubes in water exhibits a broad absorption band,[43,44] **Figure 6a**. Results of remote addressing of microcapsules containing carbon nanotubes are shown in Figure 6b,c. An optical microscope image of a microcapsule before illumination with a near-IR laser source

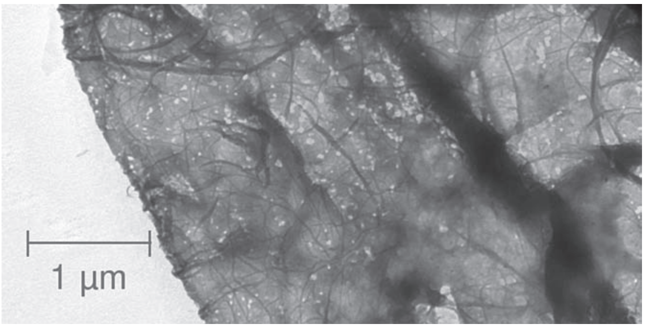

Figure 3. TEM image of a section of a microcapsule with carbon nanotubes in the walls.

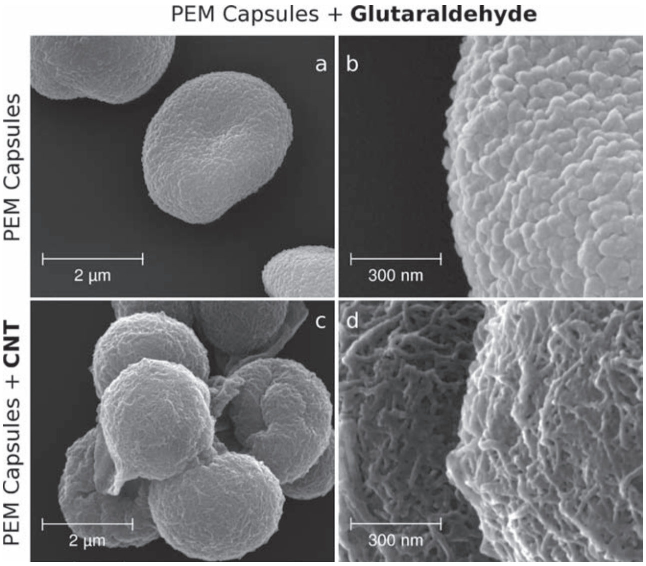

Figure 5. SEM images of microcapsules: a,b) with glutaraldehyde treatment and without carbon nanotubes; c,d) with glutaraldehyde treatment and carbon nanotubes in the microcapsule shells.

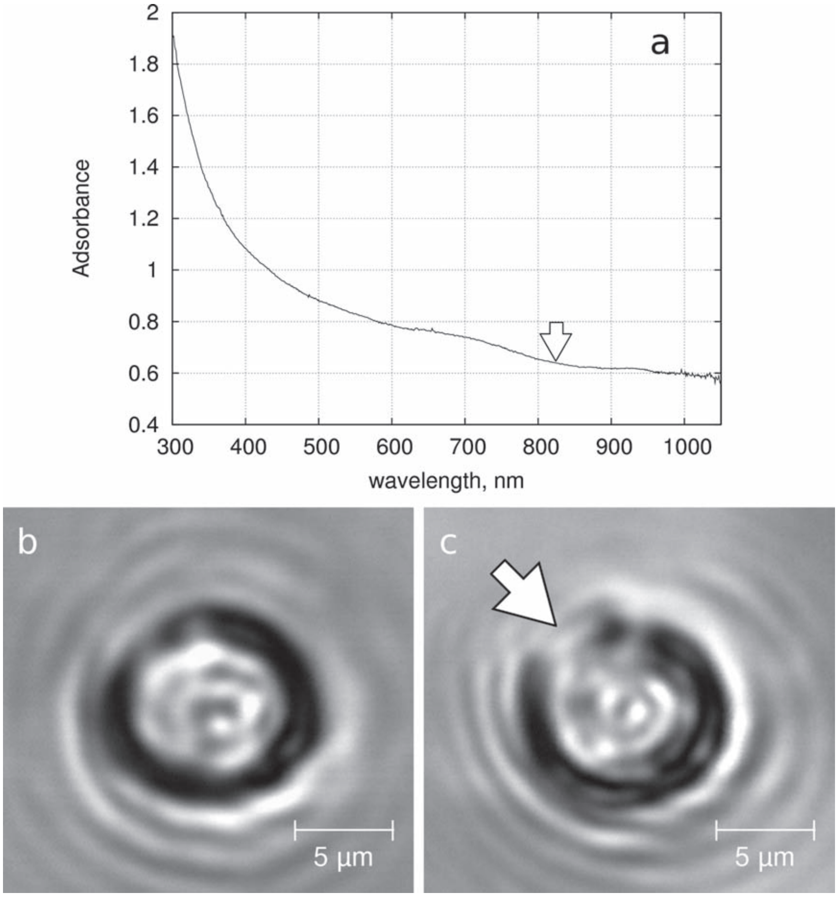

Figure 6. a) Absorption spectrum of carbon nanotubes in water. Optical microscopy images of microcapsules before (b), and after (c) near-IR laser (830 nm) activation. The scale bars in b and c correspond to 5 µm. The arrow in a indicates the laser wavelength, while the arrow in c shows the laser spot used for remote opening.

is shown in Figure 6b. The same capsule after laser illumination can be seen in Figure 6c. Although completely covered with carbon nanotubes, PEM microcapsules did not explode, but formed a small hole in the surface of the microcapsule. Deformation of microcapsules analyzed in this work resembles deformation of microcapsules with locally arranged gold nanoparticles.[45] When microcapsules with small amount of gold nanoparticles (<5% of the surface coverage) were exposed to laser light, they did not explode[31] suggesting that heat is localized.

Local opening of a microcapsule shell is the result of the temperature increase achieved during laser illumination. In accordance with Ref.[46] the temperature change is related to the heating rate per unit volume per unit time, the thermal conductivity of the surrounding medium, the size of absorbing centers, their specific heat capacity and thermal conductivity.[45] The heating rate is proportional to the incident power density, absorption of heating centers and their concentration.[46] Material parameters of carbon nanotubes and gold nanoparticles reveal that the magnitude of the extinction coefficient of gold nanoparticles at the maximum adsorption is higher than that for carbon nanotubes.[47] The specific heat capacity and thermal conductivity for gold (129 J kg^{-1} K^{-1}, 318 W mK^{-1}[48]) is lower than for the carbon nanotube (600 J kg^{-1} K^{-1},[49] 950 W mK^{-1} along the axis of the nanotube[50]), while the high surface area of carbon nanotubes due to their network distribution in the capsule shell (Figure 5c,d) can lead to an increase of heat dissipation upon laser irradiation.

Investigation by a combined AFM-Raman spectrometer setup was conducted in the next step to understand the nature of remote microcapsule activation. Before laser irradiation (473 nm) an AFM image of the capsule was collected **Figure 7a**. The Raman spectrum of the capsule wall is shown in Figure 7c, and it is characteristic for carbon nanotubes.[51] The spectrum was obtained from dried capsules with a blue CW laser (473 nm (2.62 eV), 3.5 mW power on sample).

The carbon nanotube diameter can be assessed using the following equation $d = 224/(\omega_{\mathrm{RBM}} - 14)$, where d is the diameter and ω_{RBM} is the Raman shift.[52,53] In our case the diameter of the carbon nanotube is 1.6 ± 0.1 nm.

With increasing laser power the intensity of D-band at 1335 cm^{-1} increases, the fluorescent background appears in the spectrum, and finally at a laser power of about 12 mW (100 mW µm^{-2}) the spectrum turns to the one shown in Figure 7d, which is similar to carbon black.[54] The capsule damage is clearly seen in the AFM image obtained after irradiation, Figure 7b. If the same experiment is performed in water, the maximum available laser power of 35 mW (280 mW µm^{-2}) is not high enough to obtain the same change in the Raman spectrum and a visible damage of the capsule shell. It can be noted that the mechanism proposed above for capsule laser damage differs from the one that has been demonstrated for composite carbon nanotubes/gel structure.[55] We ascribe this to the different wavelength (in two times less wavelength) and quite different power density (approximately 2000 times higher than in Ref.[55]) in our case. In Ref.[56] it was found that the threshold laser power for rapid burnout is between 400 and 900 mW µm^{-2} and the burnout depends linearly on time at lower power density of 80 mW µm^{-2}. The effect of laser irradiation on the intensity of the RBM, D, and G bands of Raman spectra of carbon nanotubes at significantly lower power densities has already been demonstrated.[57,58] Usually a decreasing intensity of RBM and G bands and an increasing of intensity of D-band is observed which is related to disorder in the nanotubes. Thus comparing the Raman spectra of CNT/polyelectrolyte before (Figure 7c) and after laser irradiation similar (Figure 7d) we arrive the same conclusion. We expected that the local temperature is higher than the temperature of nanotube decomposition (750 °C in air[59]), but a more accurate value is hard to obtain.

We believe that microcapsules studied in this work show interesting possibilities for implementation of multicompartment

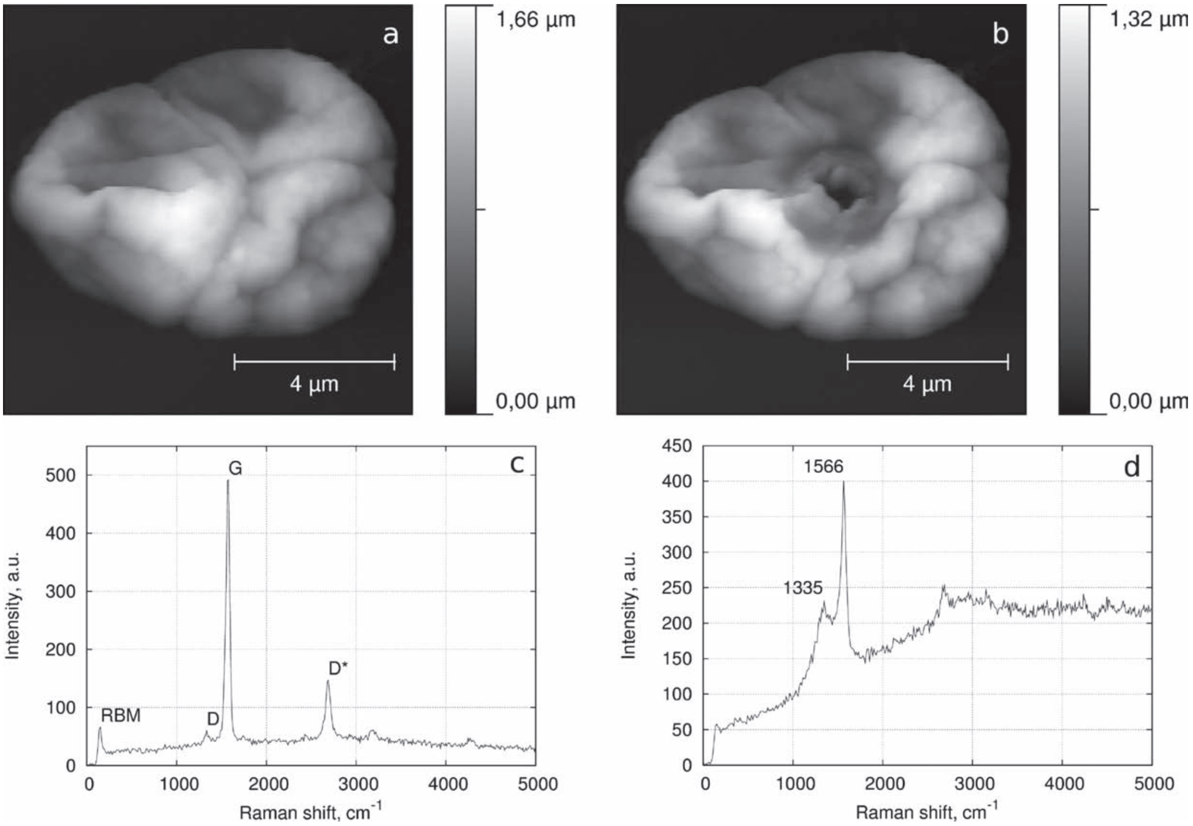

Figure 7. AFM images of microcapsules before (a) and after (b) irradiation by laser operating at 473 nm. The corresponding Raman spectra taken from the same area in the middle of the same microcapsule are presented in c and d, respectively.

microcapsules[60–62] and films[62] with selective activation. Unlike microcapsules functionalized with nanoparticles, where multiwavelength activation can be induced by aggregation of nanoparticles[31] or nanorods,[64] activation and release from microcapsules containing CNT can be initiated by laser operating at any wavelength in broad spectral range.

3. Conclusions

We have fabricated polyelectrolyte multilayer microcapsules containing carbon nanotubes in their shells. All steps of nanocomposite microcapsule formation have been characterized by SEM. Incorporation of carbon nanotubes and subsequent treatment with glutaraldehyde results in free-standing structures and these structures do not collapse after drying. The carbon nanotubes possess broad absorption in the IR and visible range. This property was used in our work for remote activation and opening of the shell by lasers operating at 473 nm and 830 nm. The Raman spectra and AFM images of microcapsule before and after laser irradiation confirm that remote laser activation is accompanied by selective local destruction of CNTs and polyelectrolyte matrix in the microcapsule shell. Thus, the microcapsules structures described here provide new opportunities for biomedical applications owing to their improved mechanical stability[10] and a point-wise manipulation with laser beams.

4. Experimental Section

Materials: Poly(sodium 4-styrenesulfonate) (PSS, MW ~ 70000 and MW ~ 1000000 Sigma), poly(allylamine hydrochloride) (PAH, MW ~ 70000, Sigma), glutaraldehyde (70% water solution) were purchased from Sigma-Aldrich-Fluka. Sodium chloride (NaCl), ethylenediaminetetraacetic acid (EDTA), calcium chloride dihydrate ($CaCl_2{\cdot}2H_2O$), and sodium carbonate (Na_2CO_3) were purchased from Merck. Purified HiPco single wall carbon nanotubes (CNT) were purchased from Carbon Nanotechnologies Inc.

Carbon Nanotube Surface Modification: In order to incorporate various amounts of functional groups into CNTs, CNTs were treated with 15.2 M HNO_3 for 2 h and 7.9 M HNO_3 for 1 h in an ultrasonic bath (VWR model 150HT). These functionalized CNTs were filtered with a PTFE membrane, rinsed with deionized water, and collected as solid powder. CNTs with carboxyl groups at the surface have been obtained as result of this treatment. This powder was redispersed in 1 mg·mL^{-1} PSS (MW ~ 1000000) water solution. To prepare a homogeneous dispersion, the mixture was sonicated overnight in ultrasonic bath. The dispersion was precipitated for several days and then the supernatant was collected to be used for LbL assembly. Instead of precipitation, a mild centrifugation can be used in order to speed up the process. However, the yield of dispersed CNTs decreases in this case because only short CNTs remain in the supernatant after centrifugation. Although each method has different advantages, the simple precipitation is preferred here for LBL assembly.

Calcium Carbonate Microparticle Preparation: Calcium carbonate ($CaCO_3$) particles were fabricated as previously published.[42] Briefly, $CaCl_2$ and Na_2CO_3 solutions (0.33 M) were mixed under vigorous stirring leading to the precipitation of $CaCO_3$ particles. The size of $CaCO_3$ particles was controlled by the duration of the steering cycle; in the current experiments in the range of 2 to 8 µm was chosen. Subsequently four centrifugation and washing steps with pure water were performed in order to remove the un-reacted components.

Core-Shell Structure and Microcapsule Fabrication: Multilayered capsules were fabricated as follows. In the first step the $CaCO_3$ microparticles were coated using the LbL technique. The first polyelectrolyte layer was made by adsorption of positively charged PAH from 2 mg·mL^{-1} solution in 0.5 M NaCl. The dispersion was continuously shaken during 15 min followed by three centrifugation/washing steps with deionised water. The second layer was prepared by absorption of negatively charged PSS from 2 mg·mL^{-1} solution in 0.5 M NaCl (15 min of shaking) followed again by three centrifugation/washing steps. This procedure was repeated four times to deposit four bi-layers on the surface of $CaCO_3$ microparticles. PSS-stabilized single wall carbon nanotube layer were formed by the LbL technique after the positively charged polyelectrolyte PAH deposition. The initial suspension of CNTs was diluted in deionised water with a ratio 1/10 (v/v). The Zeta-potential of PSS-stabilized single wall carbon nanotubes is -64.1 ± 0.2 mV. The dispersion was continuously shaken during 15 min followed by three times centrifugation and washing in deionised water. As a second step the $CaCO_3$ core was removed by complexation with EDTA. Coated $CaCO_3$ particles were shaken during 10 min with 1 mL of 0.2 M EDTA-solution followed by centrifugation and redispersion in 1 mL of fresh EDTA-solution. The obtained hollow microcapsules were washed four times with water. Thus, the shell structure of the microcapsule was $(PAH/PSS)_4/PAH/CNT$ and as control also were used microcapsules with the shell structure $(PAH/PSS)_{5.}$

Glutaraldehayde Treatment: Glutaraldehyde treatment consists of the following steps. After centrifugation and removing of supernatant about 0.5 mL of 25% glutaraldehyde was added to microcapsules and then this suspension was stored in a fridge during 1 h at 4 °C. A second step was the removal of 25% glutaraldehyde with a transfer pipette and replacement by 50% glutaraldehyde. Then the suspension was stored for 2 h at 4 °C. Finally, samples had been washed 3 times in deionized water and dried overnight at room temperature.

Microcapsules normally collapse irreversibly upon drying. Functionalization of the polyelectrolyte multilayer microcapules with carbon nanotubes and subsequent treatment with glutaraldehyde resulted in a high proportion of freestanding and non-collapsed microcapsules. Statistical evaluation showed that approximately 70% of the microcapsules maintained their shape. The criterion for a microcapsule collapse was chosen to be that the height of a microcapsule was less than half of its original diameter. Around 20 microcapsules have been used in the statistical analysis.

Methods: An Agilent-8453 (HP, UK) spectrophotometer (with pure water as the reference) was used for investigation of UV, vis, near IR absorption of carbon nanotubes.

The Zeta-potential of CNT suspensions was measured by a Zetasizer Nano-Z (Malvern Instruments Ltd, UK). Overall, 10 measurements were performed. Each result represents an average of three subsequent measurements.

SEM investigations were performed with a Quanta 200 FEG FEI scanning electron microscope operated at an acceleration voltage of 20 kV. Treatment of the samples by glutaraldehyde was used for preserving their shape upon drying. For sample preparation, a drop of the sample solution was placed onto a silicon wafer, dried in air, and sputtered with gold.

TEM images were obtained using Jeol JEM-100B and Zeiss EM 912 Omega transmission electron microscopes operating at 300 kV. The samples were prepared by deposition of an aqueous suspension of capsules onto the Formvar film supported by the copper grid. The TEM specimens were also analyzed by electron energy loss spectroscopy (EELS), in order to determine the chemical composition of nanocomposite microcapsules.

AFM images of capsules before and after laser irradiation were recorded with an Integra Spectra microscope (NTMDT, Russia) in tapping mode. For image acquisition NSG01 probes (NTMDT) with resonance frequency in the range of 115–190 kHz, force constant 2.5–10 N×m–1 and tip curvature 10 nm were used. Samples were prepared by drying a droplet of microcapsule suspension in water on a microscope glass slide.

Optical microscopy images were recorded with a Leica TCS SP confocal scanning microscope (Leica, Germany) in inverted microscope mode equipped with a 100×/1.4–0.7-oil immersion objective.

For treatment of the capsules with IR-laser radiation, the collimated laser beam of a CW laser diode at 830 nm with optical power up to 80 mW was focused onto the sample through a microscope 100x objective. Illumination was performed by a 150 W white light source and a fluorescence lamp. Images were recorded by a charge coupled device (CCD) camera connected to a computer. The solution containing capsules was deposited onto a microscope slide under the microscope objective.

Blue laser irradiation of microcapsules was performed with an INTEGRA Spectra setup. Optical microscopy images were obtained in bright field transmission mode with an Olympus IX71 microscope (part of INTEGRA Spectra setup). For imaging and laser irradiation a 100x/0.90 MPlan FL N objective was used. Optical images were captured from the video signal of the microscope camera. A solid state CW laser (wavelength 473 nm, maximum power on sample 35 mW) was used for laser irradiation through the same objective as used for imaging. For laser power regulation over a broad range a neutral density filter with variable attenuation was used. The laser power in blue laser experiments was calculated by this filter position (with an average error of 5%). Experiments with 5 microcapsules were performed.

Acknowledgements

This work was supported by the Max Planck Society and the BRIDGE Research UK Russia cooperation project-RC10, RFBR project 09–03-00245-a. A. M. Yashchenok thanks DAAD for support (Reference 325, Number A/09/03626). The authors also thank Dr. Zofia Luklinska and Mr. Mike Willis for help with SEM measurements.

Received: April 29, 2010
Published online: July 13, 2010

---

[1] S. Iijima, *Nature* **1991**, *354*, 56–58.
[2] R. H. Baughman, A. A. Zakhidov, W. A. Heer, *Science* **2002**, *297*, 787–792.
[3] P. M. Ajayan, O. Stephan, C. Colliex, D. Trauth, *Science* **1994**, *265*, 1212–1214.
[4] A. A. Mamedov, N. A. Kotov, M. Prato, D. M. Gulid, J. P. Wicksted, A. Hirsch, *Nat. Mater.* **2002**, *1*, 190–194.
[5] M. Olek, J. Ostrander, S. Jurga, H. Möhwald, N. Kotov, K. Kempa, M. Giersig, *Nano Lett.* **2004**, *4*, 1889–1895.
[6] J. N. Coleman, U. Khan, Y. K. Gun'ko, *Adv. Mater.* **2006**, *18*, 689–706.
[7] M. Moniruzzaman, K. I. Winey, *Macromolecules* **2006**, *39*, 5194–5205.
[8] P. Podsiadlo, A. K. Kaushik, E. M. Arruda, A. M. Waas, B. S. Shim, J. Xu, H. Nandivada, B. G. Pumplin, J. Lahann, A. Ramamoorthy, N. A. Kotov, *Science* **2007**, *318*, 80–83.
[9] B. S. Shim, P. Podsiadlo, D. G. Lilly, A. Agarwal, J. Lee, Z. Tang, S. Ho, P. Ingle, D. Paterson, W. Lu, N. A. Kotov, *Nano Lett.* **2007**, *7*, 3266–3273.
[10] B. S. Shim, J. Zhu, E. Jan, K. Critchley, S. Ho, P. Podsiadlo, K. Sun, N. A. Kotov, *ACS Nano* **2009**, *3*, 1711–1722.
[11] Y. Saito, S. Uemura, *Carbon* **2000**, *38*, 169–182.
[12] A. Javey, H. Kim, M. Brink, Q. Wang, A. Ural, J. Guo, P. Mcintyre, P. Mceuen, M. Lundstrom, H. Dai, *Nat. Mater.* **2002**, *1*, 241–246.
[13] S. Wang, E. Humphreys, S. Chung, D. Delduco, S. Lustig, H. Wang, K. Parker, N. Rizzo, S. Subramoney, Y. Chiang, A. Jagota, *Nat. Mater.* **2003**, *2*, 196–200.
[14] G. Dieckmann, A. Dalton, P. Johnson, J. Razal, J. Chen, G. Giordano, E. Munoz, I. Musselman, R. Baughman, R. Draper, *J. Am. Chem. Soc.* **2003**, *125*, 1770–1777.

[15] G. G. Samsonidze, E. D. Semke, M. Usrey, D. J. Walls, *Science* **2003**, *302*, 1545–1548.
[16] Y. Wang, X. Wang, B. Wu, Z. Zhao, F. Yin, S. Li, X. Qin, Q. Chen, *Sens. Actuators B* **2008**, *130*, 809–815.
[17] H. Zhao, H. Ju, *Anal. Biochem.* **2006**, *350*, 138–144.
[18] E. Miyako, H. Nagata, K. Hirano, Y. Makita, K. Nakayama, T. Hirotsu, *Nanotechnology* **2007**, *18*, 475103–475109.
[19] M. J. O'Connell, S. M. Bachilo, C. B. Huffman, V. C. Moore, M. S. Strano, E. H. Haroz, K. L. Rialon, P. J. Boul, W. H. Noon, C. Kittrell, J. Ma, R. H. Hauge, R. B. Weisman, R. E. Smalley, *Science* **2002**, *297*, 593–596.
[20] M. K. Gheith, V. A. Sinani, J. P. Wicksted, R. L. Matts, N. A. Kotov, *Adv. Mater.* **2005**, *17*, 2663–2670.
[21] G. Decher, *Science* **1997**, *277*, 1232–1237.
[22] Yu. Lvov, G. Decher, H. Möhwald, *Langmuir* **1993**, *9*, 481–486.
[23] G. B. Sukhorukov, E. Donath, S. Davis, H. Lichtenfeld, F. Caruso, V. I. Popov, H. Möhwald, *Polym. Adv. Technol.* **1998**, *9*, 759–767.
[24] D. V. Andreeva, D. A. Gorin, H. Möhwald, G. B. Sukhorukov, *Langmuir* **2007**, *23*, 9031–9036.
[25] a) D. A. Gorin, S. A. Portnov, O. A. Inozemtseva, Z. Luklinska, A. M. Yashchenok, A. M. Pavlov, A. G. Skirtach, H. Möhwald, G. B. Sukhorukov, *Phys. Chem. Chem. Phys.* **2008**, *10*, 6899–6905; b) B. G. De Geest, A. G. Skirtach, T. R. M. De Beer, G. B. Sukhorukov, L. Bracke, W. R. G. Baeyens, J. Demeester, S. C. De Smedt, *Macromol. Rapid Commun.* **2007**, *28*, 88–95.
[26] a) A. G. Skirtach, C. Déjugnat, D. Braun, A. S. Susha, A. L. Rogach, G. B. Sukhorukov, *J. Phys. Chem. C.* **2007**, *111*, 555–564; b) B. V. Parakhonskiy, M. F. Bedard, T. V. Bukreeva, G. B. Sukhorukov, H. Möhwald, A. G. Skirtach, *J. Phys. Chem. C* **2010**, *114*, 1996–2002.
[27] D. G. Shchukin, D. A. Gorin, H. Möhwald, *Langmuir* **2006**, *22*, 7400–7404.
[28] A. G. Skirtach, A. M. Javier, O. Kreft, K. Köhler, A. P. Alberola, H. Möhwald, W. J. Parak, G. B. Sukhorukov, *Angew. Chem. Int. Ed.* **2006**, *45*, 4612–4617.
[29] B. G. De Geest, S. De Koker, G. B. Sukhorukov, O. Kreft, W. J. Parak, A. G. Skirtach, J. Demeester, S. C. De Smedt, W. E. Hennink, *Soft Matter* **2009**, *5*, 282–291.
[30] R. Palankar, A. G. Skirtach, M. F. Bedard, O. Kreft, M. Garstka, K. Goude, H. Möhwald, G. B. Sukhorukov, M. Winterhalter, S. Springer, Small **2009**, *5*, 2168–2176.
[31] M. F. Bedard, D. Braun, G. B. Sukhorukov, A. G. Skirtach, *ACS Nano* **2008**, *2*, 1807–1816.
[32] M. F. Bedard, A. Munoz-Javier, R. Mueller, P. del Pino, A. Fery, W. J. Parak, A. G. Skirtach, G. B. Sukhorukov, *Soft Matter* **2009**, *5*, 148–155.
[33] A. M. Javier, O. Kreft, M. Semmling, S. Kempter, A. G. Skirtach, O. T. Bruns, P. del Pino, M. F. Bedard, J. Raedler, J. Kaes, C. Plank, G. B. Sukhorukov, W. J. Parak, *Adv. Mater.* **2008**, *20*, 4281–4287.
[34] P. A. L. Fernandes, M. Delcea, A. G. Skirtach, H. Möhwald, A. Fery, *Soft Matter* **2010**, *6*, 1879–1883.
[35] J. Cui, Y. Liu, J. Hao, *J. Phys. Chem. C.* **2009**, *113*, 3967–3972.
[36] M. A. Correa-Duarte, A. Kosiorek, W. Kandulski, M. Giersig, L. M. Liz-Marzan, *Chem. Mater.* **2005**, *17*, 3268–3272.
[37] Q. Zhao, C. Gao, J. Shen, Y. Li, X. Zhang, *Macromol. Rapid Commun.* **2004**, *25*, 2014–2018.
[38] V. N. Paunov, M. Panhuis, *Nanotechnology* **2005**, *16*, 1522–1525.
[39] M. M. Caruso, S. R. Schelkopf, A. C. Jackson, A. M. Landry, P. V. Brauna, J. S. Moore, *J. Mater. Chem.* **2009**, *19*, 6093–6096.
[40] S. J. Pastine, D. Okawa, A. Zettl, M. J. Frechet, *J. Am. Chem. Soc.* **2009**, *131*, 13586–13587.
[41] a) C. Peracchia, B. S. Mittler, *J. Cell Biol.* **1979**, *53*, 234–238; b) A. V. Sapelkin, S. C. Bazliss, B. Unal, A. Charalambou, *Biomaterials* **2006**, *27*, 842–846.
[42] D. V. Volodkin, A. I. Petrov, M. Prevot, G. B. Sukhorukov, *Langmuir* **2004**, *20*, 3398–3406.
[43] H. Yang, S. C. Wang, P. Mercier, D. L. Akins, *Chem. Commun.* **2006**, *13*, 1425–1427.
[44] G. A. Rance, D. H. Marsh, A. N. Khlobystov, *Chem. Phys. Lett.* **2008**, *460*, 230–236.
[45] A. G. Skirtach, C. Dejugnat, D. Braun, A. S. Susha, A. L. Rogach, W. J. Parak, H. Möhwald, G. B. Sukhorukov, *Nano Lett.* **2005**, *5*, 1371–1377.
[46] A. G. Skirtach, A. A. Antipov, D. G. Shchukin, G. B. Sukhorukov, *Langmuir* **2004**, *20*, 6988–6992.
[47] S. H. Jeong, K. K. Kim, S. J. Jeong, K. H. An, S. H. Lee, Z. H. Lee, *Synth. Met.* **2007**, *157*, 570–574.
[48] S. Nagasaki, *Metal Handbook*, 2nd ed., The Japan Institute of Metals, Maruzen: Tokyo, **1984**.
[49] S. P. Hepplestone, A. M. Ciavarella, C. Janke, G. P. Srivastava, *Surf. Sci.* **2006**, *600*, 3633–3636.
[50] J. Che, T. A. Cagin, W. Goddard, *Nanotechnology* **2000**, *11*, 65–69.
[51] M. S. Dresselhaus, G. Dresselhaus, R. Saito, A. Jorio, *Phys. Rep.* **2005**, *409*, 47–99.
[52] H. Huang, R. Maruyama, K. Noda, H. Kajiura, K. Kadano, *J. Phys. Chem. B* **2006**, *110*, 7316–7320.
[53] M. C. Hersam, *Nat. Nanotechnol.* **2008**, *3*, 387–394.
[54] T. Jawhari, A. Roid, J. Casado, *Carbon* **1995**, *33*, 1561–1565.
[55] T. Fujigaya, T. Morimoto, Y. Niidome, N. Nakashima, *Adv. Mater.* **2008**, *20*, 3610–3614.
[56] B. Zandian, R. Kumar, A. Bushmaker, S. B. Cronin, *Carbon* **2009**, *47*, 1292–1296.
[57] D. Olevik, A. V. Soldatov, M. B. Dossot, B. Vigolo, B. Humbert, E. McRae, *Phys. Status Solidi B* **2008**, *245*, 2212–2215.
[58] T. Ueda, S. Katsuki, N. Heidari Abhari, T. Ikegami, F. Mitsugi, T. Nakamiya *Surf. Coat. Techn.* **2008**, *202*, 5325–5328.
[59] E. T. Thostenson, C. Li, T. W. Chou, *Comp. Sci. Techn.* **2005**, *65*, 491–516.
[60] M. Delcea, A. M. Yashchenok, K. Videnova, O. Kreft, H. Moehwald, A. G. Skirtach, *Macromol. Biosci.* **2010**, *10*, 465–474.
[61] R. Chandrawati, L. Hosta-Rigau, D. Vanderstraaten, S. Lokuliyana, B. Stadler, F. Albericio; F. Caruso, *ACS Nano* **2010**, *4*, 1351–1361.
[62] B. Staedler, R. Chandrawati, K. Goldie, F. Caruso, *Langmuir* **2009**, *25*, 6725–6732.
[63] A. G. Skirtach, D. V. Volodkin, H. Möhwald, *ChemPhysChem* **2010**, *11*, 822–829.
[64] A. G. Skirtach, P. Karageorgiev, B. G. De Geest, N. Pazos-Perez, B. Braun, G. B. Sukhorukov, *Adv. Mater.* **2008**, *20*, 506–510.